

Facile Approach to Functionalize Nanodiamond Particles with V-Shaped Polymer Brushes

Jianli Cheng, Junpo He,* Changxi Li, and Yuliang Yang

Department of Macromolecular Science, Fudan University, Shanghai, 200433, China, and the Key Laboratory of Molecular Engineering of Polymers, Ministry of Education, China

Received February 4, 2008. Revised Manuscript Received April 20, 2008

Nanodiamond (ND) particles were functionalized with V-shaped polymer brushes of polystyrene and poly(*t*-butyl methacrylate) (PtBMA) through the reaction of surface carboxylic groups of NDs toward epoxy functionalities located in the middle of the polymer precursor, an ABC-type triblock copolymer. The block copolymer was prepared through sequential radical polymerizations of *t*BMA, glycidyl methacrylate (GMA), and styrene mediated by a reversible addition–fragmentation chain transfer process, in which the lengths of different segments are well-controlled by virtue of the living nature of the reaction. The polymerization product, PtBMA-*b*-PGMA-*b*-PS, carried a short block of PGMA in the middle, which was used for subsequent reaction with -COOH on the convex surface of the NDs. This grafting-onto approach through a center-linking process functionalized nanoparticles with V-shaped polymer brushes possessing an exact 1:1 molar ratio of different arms. Furthermore, ND particles with amphiphilic functionalities were prepared after hydrolysis of the PtBMA segment. The obtained polymer grafted ND was characterized by electron microscopy (TEM and SEM), NMR and IR spectroscopy, and TGA. The product not only formed stable dispersions in organic solvents such as tetrahydrofuran, toluene, and chloroform but also self-assembled at oil–water interfaces to form flat films or large droplets of water-in-oil and oil-in-water. The mechanism of self-assembly at liquid–liquid interfaces is discussed.

Introduction

Nanodiamonds (NDs) are a material of unique properties combining high surface area and super hardness of primary crystals. It is therefore of great interest, and high feasibility, to modify the surface of NDs using organic entities to compound with substrates. Nevertheless, only a limited number of studies on ND surface modification can be found in the literature. Khabashesku and co-workers¹ prepared fluoro-, alkyl-, amino-, and amino acid-functionalized NDs and used them to fabricate a ND-coated glass surface.² Krüger and co-workers³ synthesized peptide-conjugated NDs from a silanized precursor that could be useful in biological studies. Lukehart and co-workers⁴ synthesized ND polymer brushes using atom transfer radical polymerization (ATRP), in which the brush density and thickness were well-controlled.

The functionalization of nanoparticles (NPs) by organic molecules is not only an efficient way to prevent agglomeration of NPs in a solvent or matrix⁵ but also is a way to direct the assembly of NPs at liquid–liquid interfaces to fabricate two-dimensional structures or to form encapsulations of

water-in-oil (w/o) and oil-in-water (o/w) solutions.⁶ The assembly of NPs at interfaces can be achieved either by controlling the wettability of NPs around 90°, like that in Pickering emulsions,⁷ or by grafting the NPs with polymers.⁸ For example, Russell et al.^{9a} and Emrick et al.^{9b} functionalized the surface of cadmium selenide (CdSe) NPs with tri-*n*-octylphosphine oxide (TOPO). TOPO covered CdSe adsorbed to the interface of water and toluene and underwent transportation across the interface when the ligand was exposed to light. The assembly was further cross-linked to

* Corresponding author. Fax: +86-21-6564-0293; e-mail: jphe@fudan.edu.cn.

- (1) (a) Liu, Y.; Gu, Z. N.; Margrave, J. L.; Khabashesku, V. N. *Chem. Mater.* **2004**, *16*, 3924–3930. (b) Khabashesku, V. N.; Margrave, J. L.; Barrera, E. V. *Diamond Relat. Mater.* **2005**, *14*, 859–866.
- (2) Liu, Y.; Khabashesku, V. N.; Halas, N. J. *J. Am. Chem. Soc.* **2005**, *127*, 3712–3713.
- (3) Krüger, A.; Liang, Y. J.; Jarre, G.; Stegk, J. *J. Mater. Chem.* **2006**, *16*, 2322–2328.
- (4) Li, L.; Davidson, J. L.; Lukehart, C. M. *Carbon* **2006**, *44*, 2308–2315.

- (5) (a) von Werne, T.; Patten, T. E. *J. Am. Chem. Soc.* **1999**, *121*, 7409–7410. (b) Mayya, K. S.; Schoeler, B.; Caruso, F. *Adv. Funct. Mater.* **2003**, *13*, 183–188. (c) Zhang, M. M.; Liu, L.; Zhao, H. Y.; Yang, Y.; Fu, G. Q.; He, B. L. *J. Colloid Interface Sci.* **2006**, *301*, 85–91. (d) Li, D. X.; He, Q.; Cui, Y.; Li, J. B. *Chem. Mater.* **2007**, *19*, 412–417.
- (6) (a) Wang, D. Y.; Duan, H. W. M. M. *Soft Matter* **2005**, *1*, 412–416. (b) Binder, W. H. *Angew. Chem., Int. Ed.* **2005**, *44*, 5172–5175.
- (7) (a) Binks, B. P.; Lumdsdon, S. O. *Langmuir* **2000**, *16*, 8622–8631. (b) Binks, B. P.; Clint, J. H. *Langmuir* **2002**, *18*, 1270–1273. (c) Binks, B. P. *Curr. Opin. Colloid Interface Sci.* **2002**, *7*, 21–41. (d) Binks, B. P.; Clint, J. H.; Fletcher, P. D. I.; Lees, T. J. G.; Taylor, P. *Langmuir* **2006**, *22*, 4100–4103.
- (8) (a) Binks, B. P.; Murakami, R.; Armes, S. P.; Fujii, S. *Langmuir* **2006**, *22*, 2050–2057. (b) Binks, B. P.; Murakami, R.; Armes, S. P.; Fujii, S.; Schmid, A. *Langmuir* **2007**, *23*, 8691–8694. (c) Binks, B. P.; Murakami, R.; Armes, S. P.; Fujii, S. *Angew. Chem., Int. Ed.* **2005**, *44*, 4795–4798. (d) Amalvy, J. I.; Unali, G. F.; Li, Y.; Granger-Bevan, S.; Armes, S. P.; Binks, B. P.; Rodrigues, J. A.; Whitby, C. P. *Langmuir* **2004**, *20*, 4345–4354.
- (9) (a) Lin, Y.; Skaff, H.; Emrick, T.; Dinsmore, A. D.; Russell, T. P. *Science (Washington, DC, U.S.)* **2003**, *299*, 226–229. (b) Lin, Y.; Böker, A.; Habib, S.; Dinsmore, A. D.; David, C.; Emrick, T.; Thomas, P. R. *Langmuir* **2005**, *21*, 191–194.

fabricate ultrathin films¹⁰ and capsules¹¹ that exhibited mechanical strength. Very recently, the same research group covered gold NPs with segmented¹² and mixed ligands,¹³ respectively, that formed microcapsules of toluene-in-water or water-in-toluene solutions driven by the self-assembly of NPs at the interfaces. Wang and co-workers¹⁴ succeeded in controlling the contact angle of gold and silver NPs close to 90° by covering the particle surface with 2-bromopropionate groups. The resulting nanoparticles self-assembled into a monolayer at the water–toluene interface to form large water droplets. The same coverage also led to the formation of a magnetic colloidosome composed of Fe₃O₄ nanoparticles.¹⁵ Wei and co-workers¹⁶ reported the preparation of arrays organized by large gold NPs covered by resorcinarene tetrathiol, a ligand with four short hydrocarbon chains per molecule. On the other hand, Zhao and co-workers¹⁷ prepared “hairy” silica NPs covered by mixed homopolymer chain brushes polymerized from asymmetric Y-shaped initiators planted on the surface of the particles. Zubarev and co-workers grafted¹⁸ V-shaped arms of polybutadiene or polystyrene and poly(ethylene oxide) (PEO) segments onto gold nanoparticles. These amphiphilic nanoparticles exhibited a unique ability to disperse in many solvents with different polarities.¹⁷ In contrast to those NPs covered by small molecular ligands, it seems that the dispersing properties of gold NPs grafted with polymer chains were mainly controlled by the attached polymers since they were able to aggregate into a worm-like assembly in selective solvents¹⁸ and LB monolayers at the air–water and air–solid interfaces.¹⁹

We report here the functionalization of NDs using an ABC-type block copolymer of *t*-butyl methacrylate (*t*BMA), glycidyl methacrylate (GMA), and styrene prepared through controlled/living radical polymerization mediated by a reversible addition–fragmentation chain transfer (RAFT) process. The block copolymer carried a short segment of GMA in the middle of the chain that subsequently reacted with the carboxyl group on the surface of the ND. This center-linking approach facilitated the attachment of V-shaped brushes on the particle surface. After hydrolysis of the *t*BMA segment, the functionalized NDs self-assembled at the oil–water interfaces to form stable large droplets or ultrathin films.

- (10) Lin, Y.; Skaff, H.; Böker, A.; Dinsmore, A. D. *J. Am. Chem. Soc.* **2003**, *125*, 12690–12691.
- (11) Skaff, H.; Lin, Y.; Tangirala, R.; Breitenkamp, K.; Böker, A.; Russell, T. P.; Emrick, T. *Adv. Mater.* **2005**, *17*, 2082–2086.
- (12) Glogowski, E.; Tangirala, R.; He, J.; Russell, T. P.; Emrick, T. *Nano Lett.* **2007**, *7*, 389–393.
- (13) Glogowski, E.; He, J.; Russell, T. P.; Emrick, T. *Chem. Commun. (Cambridge, U.K.)* **2005**, 4050–4052.
- (14) Duan, H.; Wang, D.; Kurth, D. G.; Möhwald, H. *Angew. Chem., Int. Ed.* **2004**, *43*, 5639–5642.
- (15) Duan, H.; Wang, D.; Sobal, N. S.; Giersig, M.; Kurth, D. G.; Möhwald, H. *Nano Lett.* **2005**, *5*, 949–952.
- (16) Kim, B.; Tripp, S. L.; Wei, A. *J. Am. Chem. Soc.* **2001**, *123*, 7955–7956.
- (17) Li, D.; Sheng, X.; Zhao, B. *J. Am. Chem. Soc.* **2005**, *127*, 6248–6256.
- (18) (a) Zubarev, E. R.; Xu, J.; Sayyad, A.; Gibson, J. D. *J. Am. Chem. Soc.* **2006**, *128*, 4958–4959. (b) Zubarev, E. R.; Xu, J.; Sayyad, A.; Gibson, J. D. *J. Am. Chem. Soc.* **2006**, *128*, 15098–15099.
- (19) Genson, K. L.; Holzmueller, J.; Jiang, C.; Xu, J.; Gibson, J. D.; Zubarev, E. R.; Tsukruk, V. V. *Langmuir* **2006**, *22*, 7011–7015.

Experimental Procedures

Chemicals. Styrene (St, Shanghai Chemicals Co. Ltd., 99%), GMA (TCI, 95%), and *t*BMA (TCI, 99%) were distilled before use. All solvents (Feida Chemicals) (e.g., benzene (99.5%), tetrahydrofuran (THF, 99.5%), chloroform (99.5%), and *N,N'*-dimethylformamide (DMF, 99.0%)) were dried over CaH₂ and distilled over Na/benzophenone. 2,2'-Azobis(isobutyronitrile) (AIBN, Shanghai Fourth Factory of Chemicals, 99%) was recrystallized from methanol. Trifluoroacetic acid (TFA, Acros, >99.0%), triethylamine (TEA, Shanghai Reagents Company, 99%), HNO₃ (Shanghai Chemicals, 65–68%), and H₂SO₄ (Shanghai Chemicals, 98%) were used as received. Cumyl dithiobenzoate (CDB, 99.0%) was prepared according to the literature.²⁰ NDs (>95%, diameter 3.2 nm, Diamond Source Co. Ltd.) and dodecylamine (Shanghai Chemicals Co. Ltd., 99%) were used as received.

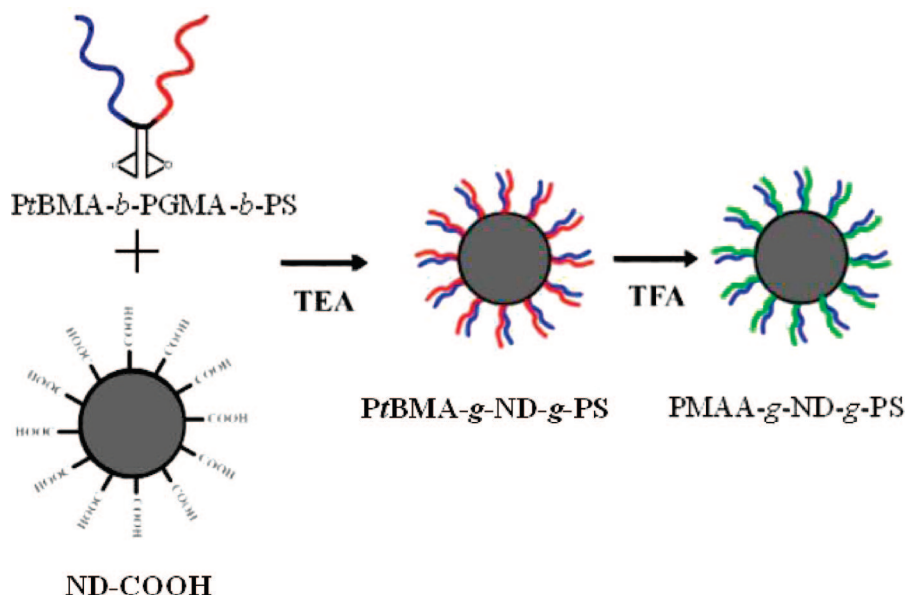
Measurements. Gel permeation chromatography (GPC) was performed on a Waters 410 system equipped with three TSK-GEL H-type columns (particle size: 5.0 μm and *M_w* range: 0–10³ and 0–2 × 10⁴ g/mol and particle size: 6.0 μm and *M_w* range: 0–4 × 10⁵ g/mol), a Waters 410 RI detector, and a Waters 486 UV detector (254 nm), using THF as the eluent at a flow rate of 1 mL/min at 40 °C. The columns were calibrated by narrow polystyrene (*M_w* range: 200–3 × 10⁶ g/mol) standards. TGA was conducted on a Netzsch TG-209 instrument under a nitrogen atmosphere (20 mL/min). The temperature was elevated from 30 to 650 °C at a rate of 20 °C/min. The TGA curve shows clearly two stages of weight loss, that of 230 to ~450 °C being for polymer content. ¹H NMR measurements were carried out on a Bruker (500 MHz) NMR instrument, using CDCl₃ as the solvent and tetramethylsilane (TMS) as the reference. IR spectra were obtained on a Magna-550 FTIR instrument (KBr pellet). High-resolution transmission electron microscopy (HR-TEM) images were recorded on a JEOL JEM2010 electron microscope operating at 200 kV. The specimens for TEM observations were prepared by placing one drop of the sample on a copper grid coated with carbon. Scanning electron microscopy (SEM) images were recorded on a Philips XL30 FEG instrument (accelerating voltage: 20 kV), and the samples were loaded on freshly cleaved mica surface and subsequently sputter-coated with a homogeneous gold layer for charge dissipation. The nanoparticle size was measured on a laser light scattering instrument (Malvern Autosizer 4700) equipped with a multi-τ digital time correlator (Malvern PCS7132) and a diode-pumped, solid-state continuous wave laser (Compass 315M-100, Coherent, Inc.; output power > 100 mW, λ₀ = 532 nm) as the light source. Photos of the interfacial assemblies were taken with a digital camera (Kodak Z7590).

Preparation of ND-COOH. Surface oxidization of NDs (1.00 g) was performed in a 120 mL mixture of concentrated sulfuric and nitric acids (3:1 v/v, 98 and 70%, respectively) at 140 °C for 12 h. The reaction mixture was diluted with deionized water, and the product, ND-COOH, was collected by a centrifuge at 7200 rpm. After thorough washing with deionized water, ND-COOH was dried in a vacuum at room temperature for 48 h.

The content of -COOH was determined by grafting dodecylamine following Shapter et al.'s method.²¹ A mixture of ND-COOH (70 mg) and dodecylamine (6.0 g, 0.03 mol) was sonicated for 1 h at 70 °C and then stirred at 110 °C for 3 days. After the reaction mixture was cooled to room temperature, ethanol (100 mL) was added, and the mixture was sonicated for 30 min, followed by centrifuging at 7200 rpm. The product was washed with ethanol

- (20) Le, T. P. T.; Moad, G.; Rizzardo, E.; Thang, S. H. PCT International Patent Application WO 9801478 A1 980115, 1998.
- (21) Matthew, W. M.; Popa-Nita, S.; Shapter, J. G. *Carbon* **2006**, *44*, 1137–1141.

Scheme 1. Pathway for Synthesis of Polymer-Grafted ND Particles



until there was no free dodecylamine in the supernatant and dried at 50 °C under vacuum overnight.

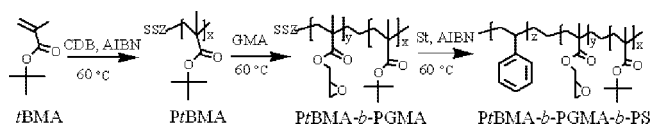
Synthesis of Triblock Copolymers PtBMA-*b*-PGMA-*b*-PS. A solution of AIBN (0.04 g, 0.25 mmol), CDB (0.13 g, 0.5 mmol), and *t*BMA (8.17 g, 57.60 mmol) in benzene (10.0 mL) was degassed by three freeze–pump–thaw cycles. The mixture was then thermostated at 60 °C under an argon atmosphere. After reaction for 10 h, GMA (5.35 g, 37.60 mmol) was added to the system by a syringe, and the reaction proceeded for a further 2 h before being quenched into liquid nitrogen. The reaction mixture was diluted with THF (5 mL) and precipitated into a mixture of methanol/water (1:1 v/v, total volume 800 mL). The product was dried under vacuum to a constant weight. $M_n = 1.23 \times 10^4$ g/mol and $M_w/M_n = 1.21$.

The resulting diblock copolymer was used as a polymeric chain transfer agent (macro-CTA) to initiate polymerization of styrene. Thus, a solution of styrene (12.7 g, 0.12 mol), macro-CTA (4.90 g, 0.40 mmol), and AIBN (0.03 g, 0.20 mmol) in benzene (12 mL) was degassed by three freeze–pump–thaw cycles. The mixture was then thermostated at 60 °C under an argon atmosphere and stopped by being quenched into liquid nitrogen at a predetermined time. The reaction mixture was diluted with THF (6 mL) and precipitated into a mixture of methanol/water (1:1 v/v, total volume 800 mL). The polymer was dried under vacuum to constant weight. $M_{n,\text{GPC}} = 2.23 \times 10^4$ g/mol and $M_w/M_n = 1.25$.

Preparation of Polymer Covered NDs, PtBMA-*g*-ND-*g*-PS. PtBMA-*b*-PGMA-*b*-PS was grafted onto NDs by the reaction of epoxy groups with a carboxyl group on the ND surface. PtBMA-*b*-PGMA-*b*-PS (2.50 g) and ND-COOH (0.40 g) were dispersed in 10 mL of DMF in a 25 mL flask by ultrasonication, after which 0.2 mL of triethylamine was added. The mixture was stirred at 120 °C for 5 days under nitrogen protection. The solid product was collected by centrifuging at 12 000 rpm. The product was washed with DMF (50 mL \times 4) until there was no polymer detected in the supernatant and then dried at 50 °C under vacuum overnight.

Hydrolysis of PtBMA Segment on Polymer Covered NDs. PtBMA-*g*-ND-*g*-PS (0.20 g) was dispersed in 20 mL of CHCl_3 by ultrasonication. TFA (0.3 g, 2.6 mmol) was added, and the mixture was stirred at room temperature for 24 h. The solvent was removed by centrifuging at 12 000 rpm. The precipitate was dried in a vacuum at 50 °C for 24 h.

Scheme 2. Synthetic Route of Triblock Copolymers



Results and Discussion

Synthesis and Characterization of Polymer Covered NDs. NDs covered with V-shaped polymer brushes were prepared by grafting an ABC-type triblock copolymer, PtBMA-*b*-PGMA-*b*-PS, onto the surface of carboxylate-functionalized ND particles (ND-COOH) by employing a reaction between epoxy and carboxyl groups, as shown in Scheme 1. This center-linking process prepared polymer brushes on NDs with an exact 1:1 molar ratio of A (PtBMA) and C (PS) arms. The pristine NDs, prepared by a detonation process, are commercially available with an average diameter of 3.2 nm (as described by the manufacturer). However, large aggregates of diameters ranging from hundreds to thousands of nanometers were observed as the main phase by TEM (vide infra). The sp^2 and sp^3 defects on the surface can be converted to carboxyl groups by acid oxidation according to a literature method.^{22,23} After reaction with $\text{HNO}_3/\text{H}_2\text{SO}_4$ (1:3 v/v) at 140 °C for 12 h, carboxylated ND particles, ND-COOH, were obtained. The content of -COOH was determined by dodecylamine grafting, a method developed by Shapter et al. for functionalized carbon nanotubes,²¹ in which an ionic bond is formed between equivalent -COOH and amine. Three parallel reactions of ND-COOH and dodecylamine gave an average content of carboxyl groups of 0.9 ± 0.1 mmol per g of ND-COOH, corresponding to ~ 3.9 wt % -COOH.

The triblock copolymer was prepared by controlled/living radical polymerization mediated by the RAFT process

(22) Aleksenskiĭ, A. E.; Baĭdakova, M. V.; Vul', A. Y.; Siklitskiĭ, V. I. *Phys. Solid State* **1999**, *41*, 668–671.

(23) Tu, J. S.; Perevedentseva, E.; Chung, P. H.; Cheng, C. L. *J. Chem. Phys.* **2006**, *125*, 174713.

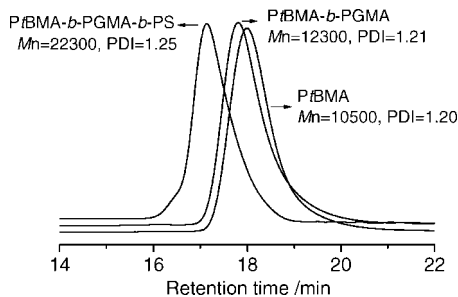


Figure 1. GPC chromatographs of triblock copolymer *Pt*BMA-*b*-PGMA-*b*-PS.

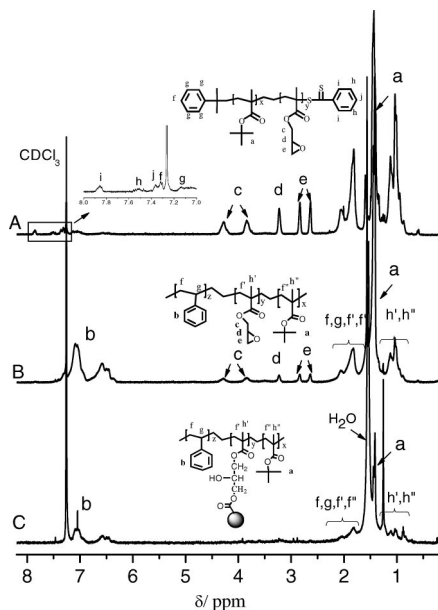


Figure 2. ^1H NMR spectra of *Pt*BMA-*b*-PGMA (A), *Pt*BMA-*b*-PGMA-*b*-PS (B), and *Pt*BMA-*b*-PGMA-*b*-PS (C).

(Scheme 2). Figure 1 shows the incremental growth of molecular weight during the reaction, indicating a living feature of polymerization. $M_{n,\text{GPC}}$ was 2.23×10^4 g/mol. The molecular weight distribution is narrow, with a polydispersity index M_w/M_n of 1.25. The ^1H NMR spectra of the sequential polymerization products are shown in Figure 2, in which A and B correspond to the intermediate diblock *Pt*BMA-*b*-PGMA and the final triblock copolymer *Pt*BMA-*b*-PGMA-*b*-PS, respectively. In the former, signals of aromatic protons of the end group (derived from the RAFT agent) are visible between 7.4 and 7.9 ppm. From integrations of the aromatic signal at 7.9 ppm and those of *t*-butyl (1.4 ppm) and epoxy (2.5–4.4 ppm) groups, the degrees of polymerization of GMA and *t*BMA are calculated to be $\text{DP}_{\text{GMA}} = 18$ and $\text{DP}_{\text{tBMA}} = 97$, respectively. The degree of polymerization of styrene (DP_{St}) is 98 as determined from the spectrum of the triblock copolymer, resulting in an estimation of $M_{n,\text{NMR}} = 2.60 \times 10^4$ g/mol.

The grafting of *Pt*BMA-*b*-PGMA-*b*-PS on ND-COOH was accomplished by a carboxylate triggered ring-opening reaction of the epoxy group located in the middle block. For a high conversion of -COOH, a 5-fold excess of the epoxy group was employed in the reaction of ND-COOH (0.40 g) and block copolymer (2.50 g). One might expect interparticle cross-linking by these multifunctional reactants. Nevertheless,

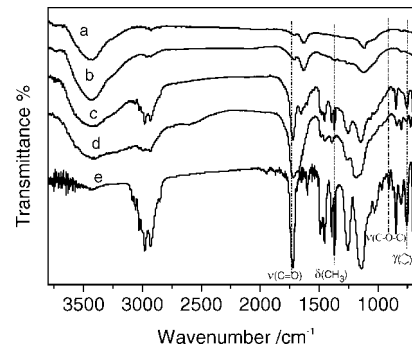


Figure 3. FT-IR spectra of pristine NDs (a), ND-COOH (b), *Pt*BMA-*g*-ND-*g*-PS (c), PMAA-*g*-ND-*g*-PS (d), and *Pt*BMA-*b*-PGMA-*b*-PS (e).

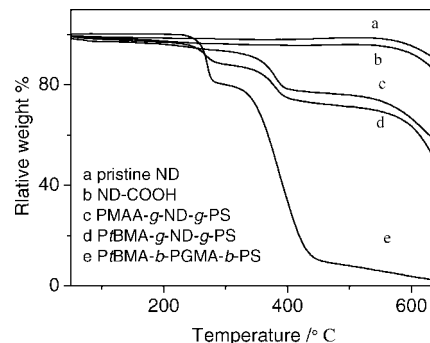


Figure 4. TGA curves of pristine NDs (a), ND-COOH (b), PMAA-*g*-ND-*g*-PS (c), *Pt*BMA-*g*-ND-*g*-PS (d), and *Pt*BMA-*b*-PGMA-*b*-PS (e).

we never observed gel formation in the reaction, even in a system in which the block copolymer intentionally was replaced by a homopolymer of GMA (homo-GMA) with a larger molecular weight $M_n = 20\,000$ g/mol (equivalent to the polystyrene standard) and $M_w/M_n = 1.20$. Thus, the absence of interparticle cross-linking is ascribed mainly to the large size of the ND aggregates and, additionally, to the short length of the GMA segment and the space hindrance of the outer blocks.

A ^1H NMR spectrum of grafted NDs, *Pt*BMA-*g*-ND-*g*-PS, is shown in Figure 2C. While aromatic and *t*-butyl protons are observed at 6.3–7.5 and 1.4 ppm, respectively, the signals of the epoxy groups disappear. This is, on one hand, due to the reaction of epoxy with carboxyl groups. On the other hand, the residual epoxy groups had a low mobility after the polymer was anchored to the surface of the ND, leading to signal broadening that makes them difficult to observe.

Figure 3 shows the FT-IR spectra of pristine NDs (a), ND-COOH (b), *Pt*BMA-*g*-ND-*g*-PS (c), hydrolyzed product PMAA-*g*-ND-*g*-PS (d), and triblock polymer *Pt*BMA-*b*-PGMA-*b*-PS (e). The bands for O-H (3450 cm^{-1}) and carboxyl group C=O (1737 cm^{-1}) became stronger after oxidation (curves a and b in Figure 3). After reaction with triblock copolymers, bands for C=O (1730 cm^{-1}), C-O (1155 cm^{-1}), the aromatic ring (755 and 694 cm^{-1}), and *t*-butyl (1360 and 1380 cm^{-1}) are clearly observed (curve c in Figure 3). The signal for the epoxy group (910 cm^{-1}) disappears after the grafting reaction due to the low content of the residual group. Efficient hydrolysis by TFA is demonstrated by the disappearance of *t*-butyl adsorption at 1360 and 1380 cm^{-1} .

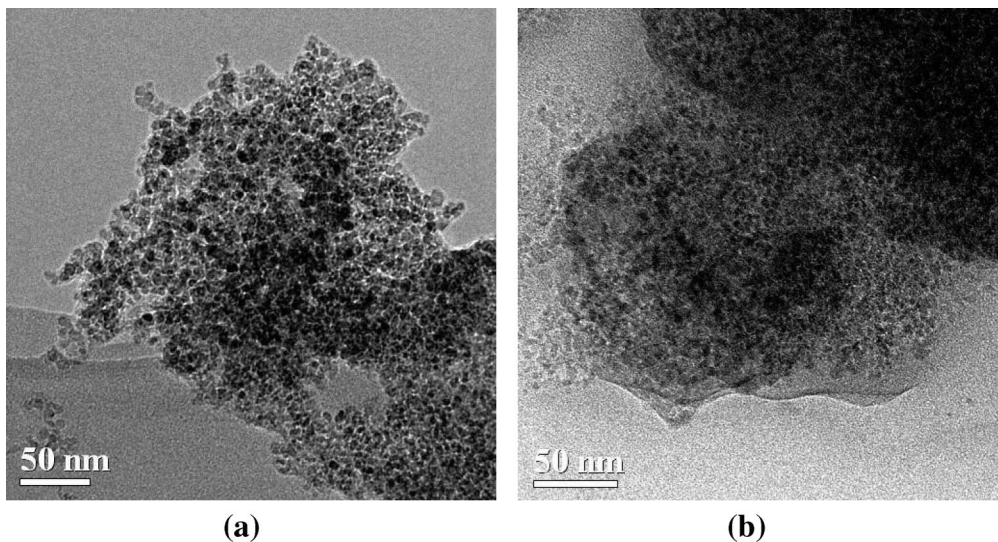


Figure 5. TEM micrographs of pristine NDs (a) and PtBMA-g-ND-g-PS (b).

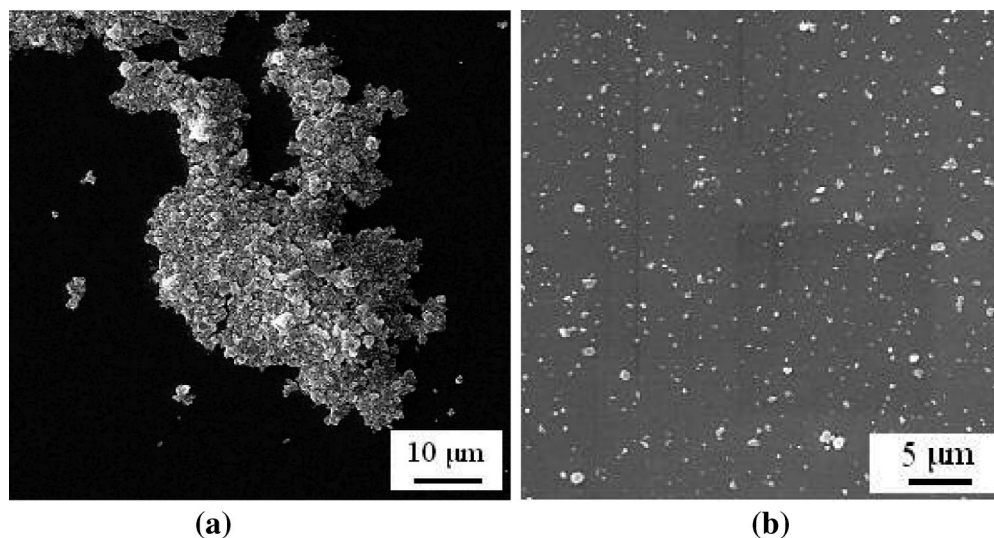


Figure 6. SEM images of pristine NDs (a) and PtBMA-g-ND-g-PS (b).

The polymer content in hybrid NDs is determined by TGA. As shown in Figure 4, the weight loss of pristine NDs at 500 °C is due to the decomposition of nondiamond carbon (sp^2), which always is observed for commercial NDs synthesized by a detonation process.²⁴ The curve of ND-COOH shows a continuous but insignificant weight loss before the decomposition of the ND itself, whereas polymer covered NDs give two decomposition stages at onset temperatures of 250 and 350 °C, which are attributable to the loss of the *t*-butyl moiety and PS/residual PtBMA segments, respectively, by correlating to TGA results of PS ($M_n = 4400$ g/mol and $M_w/M_n = 1.1$), PtBMA ($M_n = 9800$ g/mol and $M_w/M_n = 1.2$), and a mixture of PS and PtBMA (1:2 wt/wt)²⁵ (results not shown). The weight loss of *t*-butyl was not observed for the hydrolyzed product (curve c in Figure 3). From these results, the total polymer content was estimated to be around 30 wt %.

The structures of pristine and functionalized NDs also were

(24) Osswald, S.; Yushin, G.; Mochalin, V.; Kucheyev, S. O.; Gogotsi, Y. *J. Am. Chem. Soc.* **2006**, *128*, 11635–11642.

(25) Kong, H.; Gao, C.; Yan, D. *J. Mater. Chem.* **2004**, *14*, 1401–1405.

investigated by HR-TEM. TEM micrographs (Figure 5) show that ND aggregates are coated by a polymer film that is different from pristine NDs. With shielding of the polymer film, the fine nanostructure of the ND aggregates cannot be clearly identified in functionalized particles. The aggregate particle size after grafting also remarkably is reduced from several micrometers to hundreds of nanometers as shown by SEM (Figure 6). This is consistent with dynamic light scattering (DLS) results that show a mean size of 260 nm (PDI = 0.299) for PtBMA-g-ND-g-PS dispersed in THF (Figure 7).

Formation of Dispersion and Assemblies of Samples in Various Solvents. The pristine ND is insoluble in organic solvents and forms an unstable dispersion in water. After grafting with V-shaped polymer brushes, the resulting hybrid ND disperses readily in a number of organic solvents of various polarities such as THF, DMF, $CHCl_3$, and toluene (Figure 8). The dispersions are stable for at least 2 weeks followed by slow precipitation of the solid. All the dispersions display a milky color, possibly due to the presence of large clusters. After hydrolysis of the PtBMA blocks, PMAA-

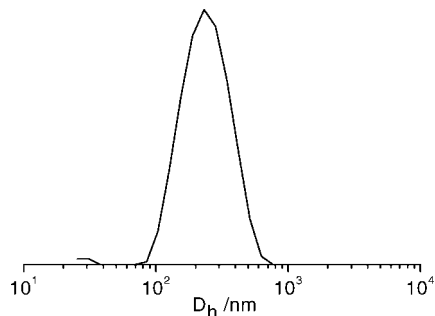


Figure 7. Size distributions of PtBMA-g-ND-g-PS particles in THF, measured by DLS.



Figure 8. Photos of dispersion status of NDs in different solvents (ca. 1 mg/mL for all samples): (A) pristine ND precipitation in THF, (B) PtBMA-g-ND-g-PS in THF, (C) PtBMA-g-ND-g-PS in DMF, (D) PtBMA-g-ND-g-PS in CHCl₃, (E) PtBMA-g-ND-g-PS in toluene, (F) PMAA-g-ND-g-PS in water, (G) PMAA-g-ND-g-PS in CHCl₃, and (H) PMAA-g-ND-g-PS in toluene.

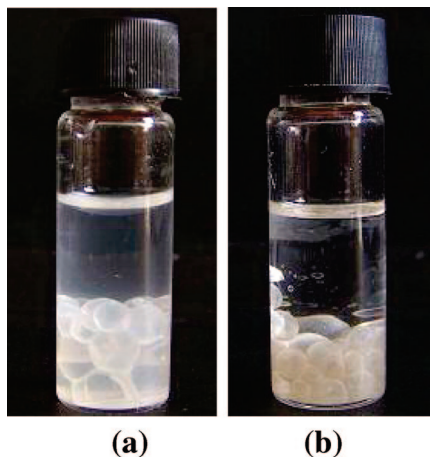


Figure 9. Photos of chloroform droplets dispersed in water (a) and water droplets dispersed in toluene (b).

g-ND-g-PS became more hydrophilic and easily was dispersed in water and organic solvents, as shown by F–H in Figure 8.

PMAA-g-ND-g-PS can be viewed as a particle grafted with amphiphilic V-shaped brushes and exhibits the ability to assemble at oil–water interfaces. In an aqueous dispersion of PMAA-g-ND-g-PS, the addition of chloroform (2:1 v/v water/chloroform) led to the formation of o/w droplets after vigorously shaking for a few seconds. Similarly, the addition of water to a dispersion in toluene resulted in w/o droplets (Figure 9) with diameters of 3 to ~5 mm. These unusually large droplets are very stable and can be stored for a period of at least 6 months. The droplets also can be removed one-by-one by using a plastic pipet due to the fluidic nature of the particle film. Figure 10a shows a system of chloroform

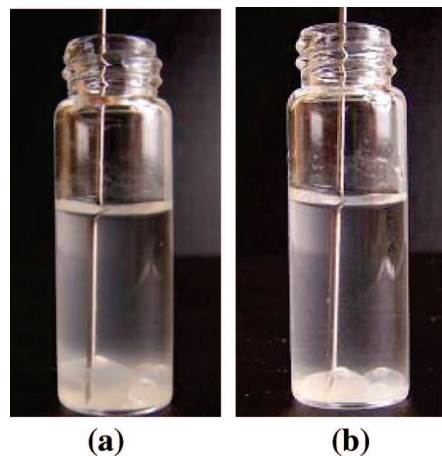


Figure 10. Photos illustrating the stability of chloroform droplets in water: (a) punctured by a needle and (b) solvent pumped out of the droplet by a syringe.

droplets in water, with only four droplets remaining after the removal of the main population while keeping the volume of water unchanged. Furthermore, a droplet can keep its shape when being punctured by a needle. Therefore, the interior content is pumped out by a syringe while the droplet shrinks but sustains a spherical or oval morphology, as shown in Figure 10b.

By optimizing the volume fraction of the solvents and the concentration of the nanoparticles, we observed a flat thin film that was adsorbed at the water–oil interface with the edge of the film creeping up the glass wall of the vial (Figure 11a). The film was transferred directly to a glass or mica substrate and investigated by TEM. Both SEM (Figure 11b) and TEM (Figure 11c) show a coarse surface formed by randomly yet closely packed nanoparticles with a broad size distribution. The large particles were formed by coagulation that may occur during the process of assembly of dispersion and/or solvent evaporation on the substrate.

There are two possible mechanisms to explain the interfacial assembly of the polymer covered ND particles. On one hand, the assembly can be regarded as interfacial adsorption driven by particle surface wettability, such as in the case of the Pickering emulsion in which the particle surface has a contact angle of $\sim 90^\circ$ at the oil–water interface.^{7,9,10} According to Binks' theory, the energy of attaching particles (ΔE) at the water–oil interface is proportional to the square of the particle diameter, d^{7c}

$$\Delta E = -\pi \left(\frac{d}{2}\right)^2 \gamma_{w/o} (1 \pm \cos\theta)^2 \quad (1)$$

in which $\gamma_{w/o}$ and θ are the tension of the water–oil interface and contact angle of particles at the interface, respectively. Thus, large particles can survive the thermal fluctuation and form a very stable assembly at the interface as long as the contact angle is $\sim 90^\circ$. Binder^{6b} calculated that a particle with $d \approx 1 \mu\text{m}$ yielded an adsorption energy $\Delta E \approx 10^7(k_B T)$ (where k_B is the Boltzmann constant and T is absolute temperature), which led to an almost irreversible adsorption at the interface. In the present work, functionalized ND particles tend to coagulate into irregularly shaped particles of $\sim 300 \text{ nm}$. It is therefore reasonable to expect a stable adsorption of ND particles at the interface, forming an

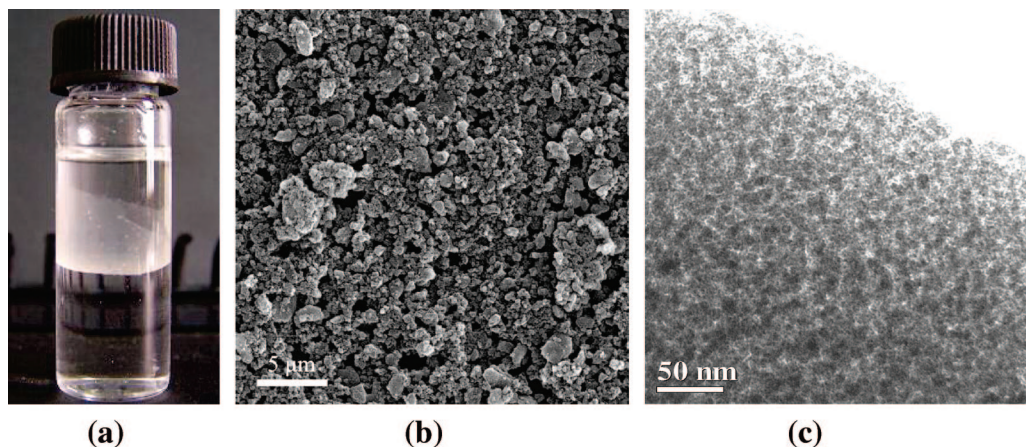


Figure 11. Photo of ND film formed at the toluene–water interface (a) and images of SEM (b) (after being transferred onto the mica substrate) and TEM (c) (after being transferred onto the carbon-coated Cu grid).

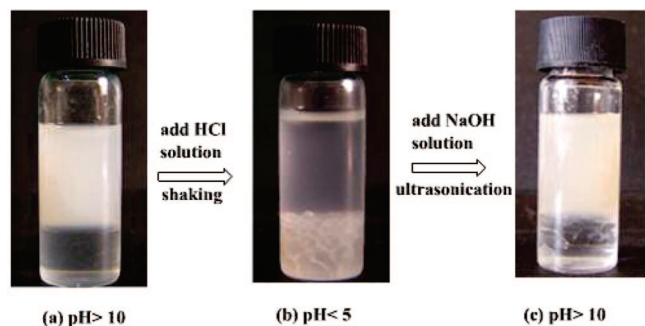


Figure 12. Photos illustrating the pH-responsive behavior of PMAA-g-ND-g-PS placed in a mixed solvent of water (upper layer) and chloroform.

emulsion upon rigorous shaking. However, the concentration of the functionalized ND particles (0.1 wt %) is low, and thus, coalescence occurs after shaking to reduce the interfacial area between oil and water and increase the interfacial concentration of the adsorbed particles, forming large oil (or water) droplets in bulk water (or oil). This is similar to the process of film formation as discussed in ref 7d. Keeping in mind that the coagulated particle size is remarkably larger than the dimension of the grafted polymer chains, we suppose that the grafting of polymers on coagulates plays a role in surface wettability modification that renders the particles able to assemble at the interface. Unfortunately, it is difficult to measure the contact angle of the particle at oil–water interfaces. On the other hand, one has to consider in the meantime the fraction of small ND particles with an average diameter of ~ 3.2 nm, which is smaller than the dimensions of polymer chains. The small particle plays a role of knot for the V-shaped chains. The resulting hybrid materials behave as star copolymers with an exactly equal number of PS and PMAA segments, which can self-assemble in solvents driven by amphiphilicity of the hybrid star copolymers. At present, we cannot determine as to what extent these two mechanisms contribute to the morphology because it is difficult to measure the fractions of large aggregates and small particles. Nonetheless, we suppose that the first mechanism is predominant because of the abundance of large aggregates as observed by TEM and the similarity of morphology to that reported by Russell^{9a,11} and Wang.^{14,15}

The polymer grafted ND is sensitive to pH changes due to the presence of the PMAA segment. As shown in Figure 12, when the pH > 10, the particle only stays in the water phase due to the larger hydrophilicity of the ionized carboxyl groups. After adjusting the pH to < 5 using a HCl solution, the polymer became less hydrophilic so that the particle preferred to reside at the interface, forming o/w droplets. Further addition of NaOH to pH > 10 followed by ultrasonication broke the droplets and led to redispersion of the grafted ND into the water phase.

Conclusion

ND particles covered by V-shaped brushes were prepared via a graft-onto approach, in which an ABC-type block copolymer, *PtBMA-b-PGMA-b-PS*, was grafted onto a ND surface by a center-linking process. The approach resulted in a relatively high functionalization efficiency, as demonstrated by TEM, SEM, ¹H NMR, and TGA, possibly due to the many reaction sites on the surface of NDs and along the middle segment of the block copolymers. The resulting polymer hybrid ND formed stable dispersions in various organic solvents in contrast to pristine NDs. Furthermore, the *PtBMA* segment was hydrolyzed to prepare an amphiphilic hybrid that was able to self-assemble at oil–water interfaces to form stable large droplets and flat films. We propose that the self-assembly is due to a wettability of $\sim 90^\circ$ of the large particle aggregates at the interfaces, although the contribution of amphiphilic star copolymers knotted by small particles cannot be excluded. The center-linking approach can be used for the functionalization of various kinds of nanoparticles, nanotubes, and nanorods. Therefore, the present work explores a general way to functionalize nano-objects with mixed polymer brushes possessing an exact equal molar amount of the two arms.

Acknowledgment. This work was subsidized by the National Basic Research Program of China (2005CB623800). J.H. and Y.Y. thank the MOE for FANEDD (200324) and the NSFC program “Excellence in Research Groups” (20221402). J.H. thanks Professor Zhijun Zhang for helpful discussions.